TLR3 deficiency renders astrocytes permissive to herpes simplex virus infection and facilitates establishment of CNS infection in mice

Line S. Reinert,[1] Louis Harder,[1] Christian K. Holm,[1] Marie B. Iversen,[1] Kristy A. Horan,[1] Frederik Dagnæs-Hansen,[1] Benedicte P. Ulhøi,[2] Thomas H. Holm,[3] Trine H. Mogensen,[4] Trevor Owens,[3] Jens R. Nyengaard,[5] Allan R. Thomsen,[6] and Søren R. Paludan[1]

[1]Department of Biomedicine, Aarhus University, Aarhus, Denmark. [2]Department of Pathology, Aarhus University Hospital, Nørrebrogade, Aarhus, Denmark. [3]Institute of Molecular Medicine, University of Southern Denmark, Odense, Denmark. [4]Department of Infectious Diseases, Aarhus University Hospital Skejby, Aarhus, Denmark. [5]Stereology and Electron Microscopy Laboratory, Centre for Stochastic Geometry and Advanced Bioimaging, Aarhus University Hospital, Aarhus, Denmark. [6]Department of International Health, Immunology and Microbiology, University of Copenhagen, Copenhagen, Denmark.

Herpes simplex viruses (HSVs) are highly prevalent neurotropic viruses. While they can replicate lytically in cells of the epithelial lineage, causing lesions on mucocutaneous surfaces, HSVs also establish latent infections in neurons, which act as reservoirs of virus for subsequent reactivation events. Immunological control of HSV involves activation of innate immune pattern-recognition receptors such as TLR3, which detects double-stranded RNA and induces type I IFN expression. Humans with defects in the TLR3/IFN pathway have an elevated susceptibility to HSV infections of the CNS. However, it is not known what cell type mediates the role of TLR3 in the immunological control of HSV, and it is not known whether TLR3 sensing occurs prior to or after CNS entry. Here, we show that in mice TLR3 provides early control of HSV-2 infection immediately after entry into the CNS by mediating type I IFN responses in astrocytes. *Tlr3*$^{-/-}$ mice were hypersusceptible to HSV-2 infection in the CNS after vaginal inoculation. HSV-2 exhibited broader neurotropism in *Tlr3*$^{-/-}$ mice than it did in WT mice, with astrocytes being most abundantly infected. *Tlr3*$^{-/-}$ mice did not exhibit a global defect in innate immune responses to HSV, but astrocytes were defective in HSV-induced type I IFN production. Thus, TLR3 acts in astrocytes to sense HSV-2 infection immediately after entry into the CNS, possibly preventing HSV from spreading beyond the neurons mediating entry into the CNS.

Introduction

Herpes simplex virus 1 (HSV-1) and HSV-2 are human pathogenic viruses, which can replicate lytically in cells of the epithelial lineage and cause mucocutaneous lesions, as seen during orofacial and genital herpes (1). Importantly, HSV-1 and HSV-2 are also neurotropic viruses and establish latent infection in neurons, which can thus serve as reservoirs of virus during subsequent events of reactivation. Due to their neurotropism, HSVs can invade the CNS and cause disease, especially in immunocompromised individuals. HSV-1 is a major cause of encephalitis, whereas HSV-2 can give rise to meningitis as well as encephalitis, sacral radiculitis, and myelitis (1, 2).

Immunological control of HSV involves both the innate and adaptive immune system, with important roles ascribed to type I IFN, natural killer cells, and CD8$^+$ T cells (3–7). Pattern-recognition receptor (PRR) activation stimulates expression of inflammatory and antimicrobial genes, such as *TNFA* and type I *IFN*, respectively (8). HSV is sensed by a series of PRRs, including TLR3, which detects double-stranded RNA (9–13). In addition to TLRs, it has been demonstrated that HSV nucleic acids are detected in the cytoplasm of infected cells and induce IFN (14–17). The physiological importance of cytoplasmic sensing of HSV remains unexplored.

The potential role of TLR3 in viral CNS infections has been addressed in several studies. TLR3 is upregulated in the CNS during viral infections, including human immunodeficiency virus encephalitis and rabies virus infection (18, 19). However, the role of TLR3 appears to differ depending on the virus and the infection model (20–22), and the emerging picture is that TLR3 can play both protective and pathological roles. For instance, there is evidence for TLR3 playing critical roles in protection against West Nile virus encephalitis, but there is also evidence that this PRR drives breakdown of the blood-brain barrier during infection with the same virus and potentiates immunopathology (20, 21). In a series of publications, Casanova, Zhang, and associates have identified and described patients with defects in the TLR3/IFN axis, all of whom had HSV-1 encephalitis, without a history of elevated susceptibility to other infections (5, 23–25). These studies indicate that, in case of HSV-1 infection in childhood, TLR3-mediated antiviral responses are needed for protection of the CNS but are redundant for host defense in the periphery. This work was followed by a case report on a patient with TLR3 deficiency, who experienced repeated reactivation of HSV-2 and development of Mollaret meningitis (26). Thus, clinical data suggest a key role for TLR3 in control of HSV infections in the CNS. However, the cells that sense HSV in a TLR3-dependent manner and activate essential defense actions in vivo remain unknown. In addition, it has not been established whether the role of TLR3 in defense against HSV infections occurs prior to

Conflict of interest: The authors have declared that no conflict of interest exists.
Citation for this article: *J Clin Invest.* 2012;122(4):1368–1376. doi:10.1172/JCI60893.

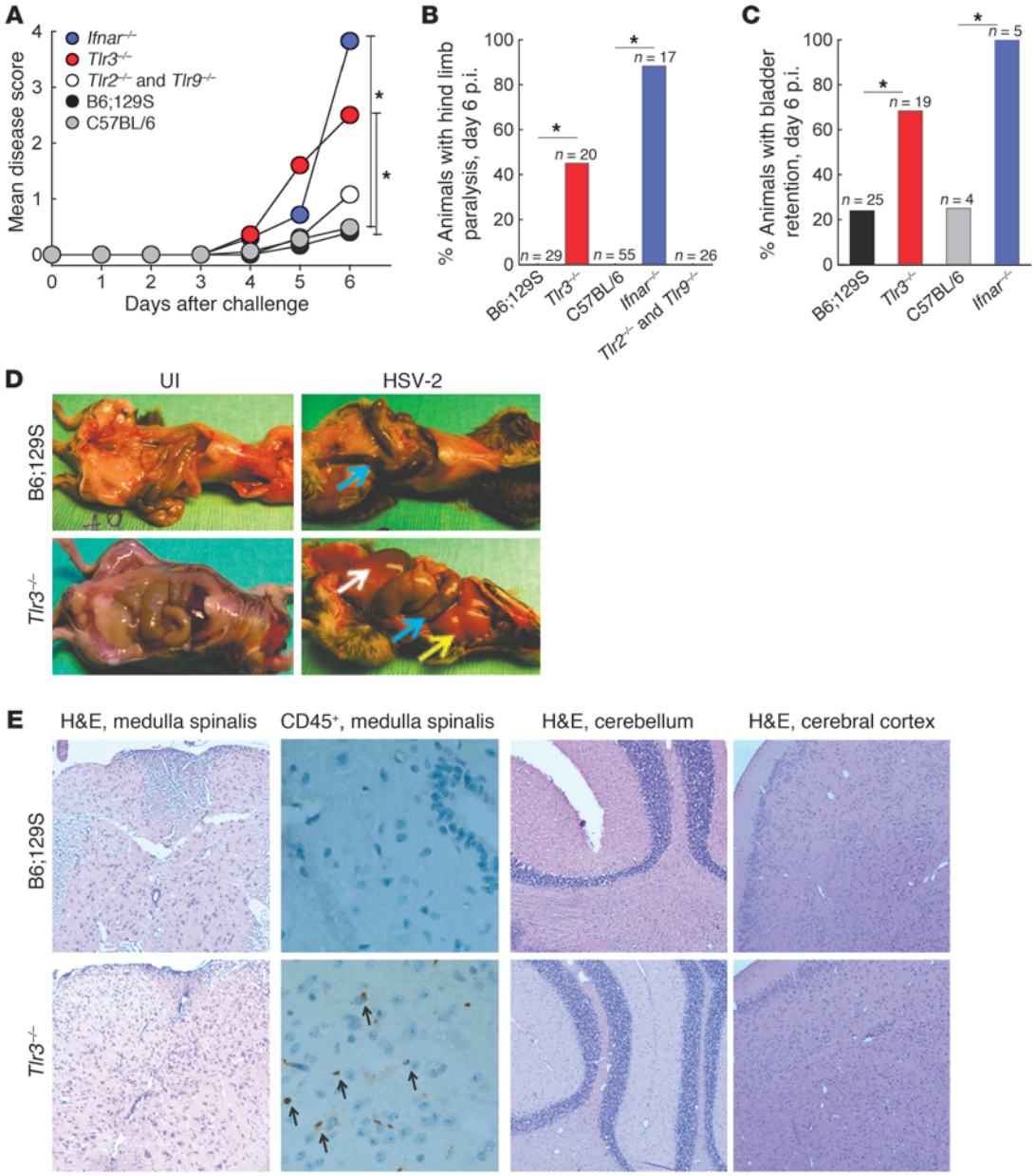

Figure 1

Tlr3$^{-/-}$ mice are hypersusceptible to HSV-2 infection. Disease development after intravaginal infection with HSV-2 (6.7×10^4 PFU). (**A**) Clinical score of infected mice from day 1–6 p.i. (**B**) Percentage of animals with hind limb paralysis on day 6 p.i. (**C**) Percentage of animals with bladder retention on day 6 p.i. (**D**) Post-mortem urinary retention (white arrow), constipation (blue arrow), and fatty liver (yellow arrow) were observed in the infected *Tlr3*$^{-/-}$ mice. (**E**) H&E-stained medulla spinalis (original magnification, ×200), cerebellum and cerebrum sections (original magnification, ×40) of infected mice day 6 p.i. Second column: staining of medulla spinalis sections with anti-CD45. CD45$^+$ cells are indicated by black arrow (original magnification: ×400). The data shown in (**A**–**C**) are mean of 3–5 independent experiments on day 6 p.i. (n = 4–12 mice in each group per experiment), and (**D**) are representative pictures of these experiments. *$P < 0.05$.

neuro-entry or within the CNS. In this work, we report that TLR3 is responsible for early control of HSV-2 after entry into the CNS by mediating the IFN-β response in astrocytes, hence limiting viral replication in neurons and restricting HSV to this cell type.

Results

Mice deficient in TLR3 or the type I IFN system are hypersusceptible to HSV-2 infection in the CNS after vaginal infection. To examine the role of TLR3 in prevention of HSV infections in mice, we infected *Tlr3*$^{-/-}$ mice with HSV-2 via the vagina. We observed a striking defect in preventing disease development in these mice as compared with that in WT control mice (on a B6;129S background) (Figure 1A), and this closely resembled the development of disease in HSV-2–infected Ifn-α receptor–deficient (*Ifnar*$^{-/-}$) mice, which were on C57BL/6 background. In these experiments, WT mice of each strain exhibited the same degree of disease. Importantly, we

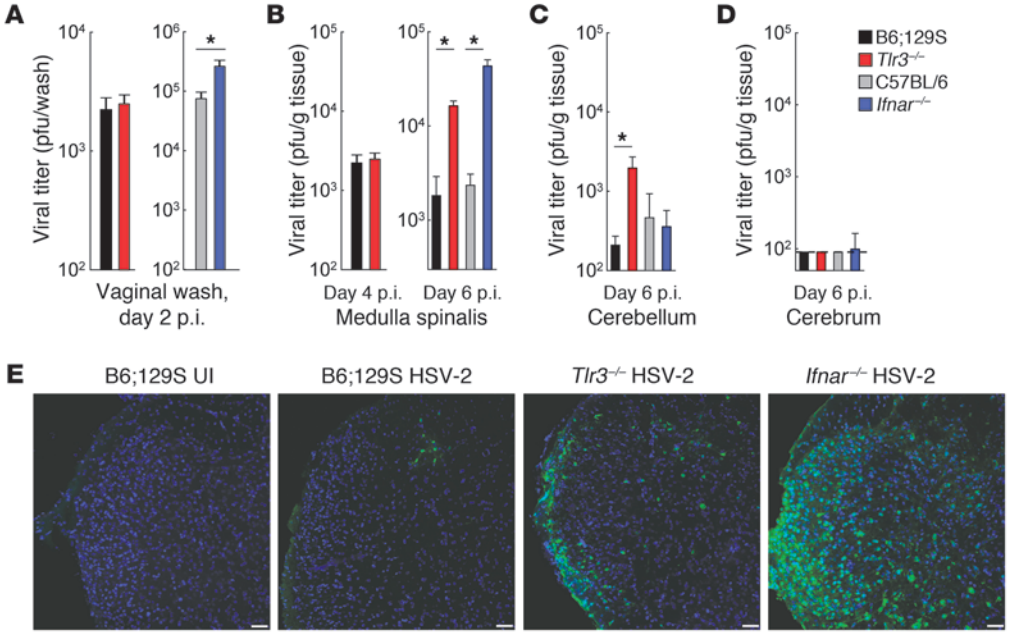

Figure 2

Tlr3$^{-/-}$ and *Ifnar*$^{-/-}$ mice have elevated viral load in the medulla spinalis on day 6 p.i. The mice were infected intravaginally with HSV-2 (6.7×10^4 PFUs). (**A**) Vaginal washes were harvested for quantification of viral load on day 2 p.i. (**B**) Viral load in the medulla spinalis on days 4 and 6. (**C**) Viral load in the cerebellum on day 6 p.i. (**D**) Viral load in the cerebrum on day 6 p.i. The dashed line indicates the detection limit. (**E**) Confocal images of the dorsal part of lumbar medulla spinalis from uninfected or infected mice (6 day p.i.). Positive anti–HSV-2 antibody staining is shown in green and nuclear staining with DAPI is shown in blue. Scale bar: 50 μm. The data are presented as mean of 3 independent experiments (n = 4–6 mice in each group per experiment). *$P < 0.05$.

observed that *Tlr3*$^{-/-}$ and *Ifnar*$^{-/-}$ mice exhibited particularly strong signs of disease in the CNS, with hind limb paralysis and urinary retention (Figure 1, A–D, and Supplemental Figure 1; supplemental material available online with this article; doi:10.1172/JCI60893DS1). For comparison, the development of disease in *Tlr3*$^{-/-}$ and *Ifnar*$^{-/-}$ mice was more pronounced than that in the case of *Tlr2* and *Tlr9* double-deficient mice, which we previously reported are susceptible to HSV-2 infection of the CNS after initial infection in the vagina (3, 27). In addition, IFN-λ receptor–deficient mice exhibited a phenotype indistinguishable from that of WT mice (N. Ank, unpublished observations, and ref. 3).

Microscopy examination of the mice revealed scattered leukocytes in the dorsal lower part of medulla spinalis in the *Tlr3*$^{-/-}$ mice but not in the WT mice (Figure 1E). In the same area, HSV-2–infected cells were found in the *Tlr3*$^{-/-}$ mice but not in the WT mice (Figure 2E). Very few leukocytes were observed in the meninges along the medulla spinalis of the *Tlr3*$^{-/-}$ mice. We observed no inflammation in the cerebral cortex, white matter, periventricular area, cerebellum, or the cerebral or cerebellar meninges. These findings suggest that *Tlr3*$^{-/-}$ mice develop myelitis after vaginal HSV-2 infection. Thus, TLR3 and IFNAR deficiency render mice susceptible to HSV-2–mediated disease in the CNS after initial infection in the peripheral tissue.

In order to examine how the lack of TLR3 affected control of virus, we examined the viral load in these mice at the site of infection in the periphery (vagina), the site of entry into the CNS (medulla spinalis), and potential sites of spread within the CNS (cerebellum and cerebrum). As seen in Figure 2A, there was no difference in the viral load in vaginal washes harvested on day 2 postinfection (p.i.) from WT and *Tlr3*$^{-/-}$ mice, suggesting that early control of the virus in the vagina was not dependent on TLR3. In the medulla spinalis, virus could be detected from day 4 p.i., and, again, no difference was observed between WT and *Tlr3*$^{-/-}$ mice (Figure 2B). By contrast, on day 6 p.i. we observed significantly higher HSV-2 titer in the medulla spinalis of *Tlr3*$^{-/-}$ mice as compared with that in WT mice (Figure 2B). The same was seen for *Ifnar*$^{-/-}$ mice. The virus did not spread efficiently to the cerebellum and cerebrum, although *Tlr3*$^{-/-}$ mice did exhibit a significantly elevated viral load in the cerebellum as compared with that in the WT mice (Figure 2, C and D). Staining of tissue sections of the lumbar medulla spinalis for HSV-2 confirmed extensive infection on day 6 p.i. in the *Tlr3*$^{-/-}$ and *Ifnar*$^{-/-}$ mice as compared with that in the WT mice (Figure 2E). Collectively, TLR3- and IFNAR-deficient mice are highly susceptible to HSV-2 infection in the CNS after initial infection in the vagina. TLR3 deficiency did not affect control of viral load in the vagina and early entry into the CNS. By contrast, the virus replicated to significantly higher titers within the medulla spinalis and cerebellum of TLR3-deficient mice.

TLR3-deficient mice do not have a global defect in type I IFN responses in the periphery and the CNS. TLR3 has been reported to have impact on both innate and adaptive immune responses during virus infections in the periphery and CNS (13, 20, 21, 28, 29). To look into the innate response to HSV-2 infection, we isolated medulla spinalis from mice infected with HSV-2 for 6 days and examined expression of IFNs, IFN-stimulated genes, and inflammatory genes. The infection led to strong induction of IFN-β expression and little or no induction of IFN-α expression in the WT mice (Figure 3, A and B). Interestingly, the elevated susceptibility of *Tlr3*$^{-/-}$ mice to

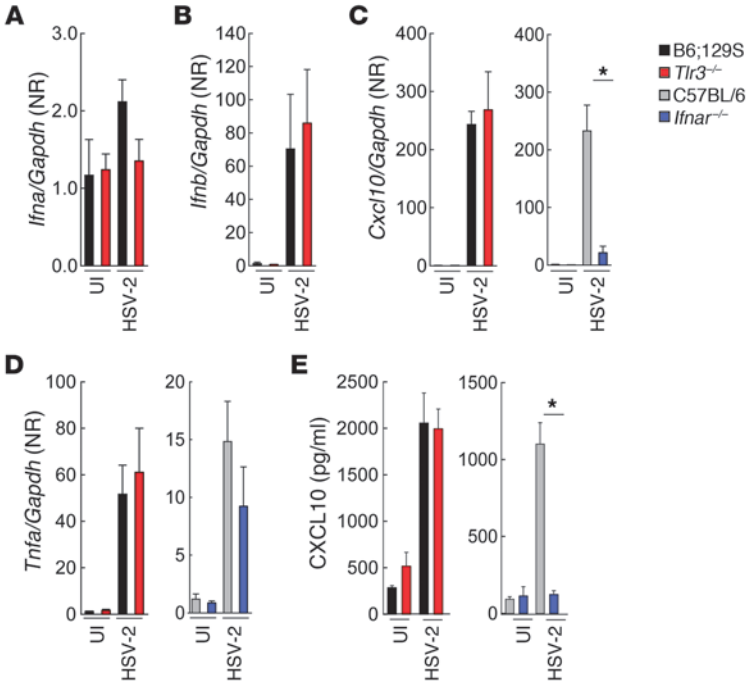

Figure 3
Expression of cytokines in medulla spinalis is unaltered in HSV-2–infected *Tlr3*$^{-/-}$ mice. (**A**–**D**) Expression of type I *Ifn*, *Cxcl10*, and *Tnfa* mRNA in the medulla spinalis of mice on day 6 after intravaginal HSV-2 infection (6.7 × 10^4 PFUs). Data are normalized to uninfected WT mice and are representative of 2–4 independent experiments (n = 5–8 mice in each group per experiment). NR, normalized ratio. (**E**) CXCL10 protein expression in vaginal wash on day 2 p.i. with HSV-2. The data are reproduced 3 times (n = 5–20 mice in each group per experiment). *P < 0.05.

HSV-2 infection in the CNS (Figures 1 and 2) was not associated with a global decrease in the expression of type I IFN (Figure 3, A and B) or IFN-stimulated genes in the CNS, as demonstrated by comparable induction of *Cxcl10* in WT and *Tlr3*$^{-/-}$ mice (Figure 3C). As expected, the *Ifnar*$^{-/-}$ mice did not induce *Cxcl10*, hence confirming this chemokine as an IFN-stimulated gene in this model (Figure 3C). The inflammatory cytokine TNF-α was also strongly induced in the CNS p.i. in a manner independent of TLR3 and IFNAR (Figure 3D). Examination of the same parameters in medulla spinalis from HSV-2–infected *Tlr2* and *Tlr9* double-deficient mice showed that the response was also independent of these PPRs (L.S. Reinert, unpublished observations), suggesting a role for other innate immune sensors in induction of the bulk of the IFN and cytokine response in the CNS during HSV-2 infection. Importantly, several PRRs reported to detect HSV infections were found to be expressed in the infected medulla spinalis and to be induced in a manner independent of TLR3 but dependent on IFNAR expression (Supplemental Figure 2), and, moreover, the CXCL10 response of microglia cells to HSV-2 infection in vitro was independent of TLR3 (Supplemental Figure 3A).

Examination of the role of TLR3 in peripheral response to HSV infection in vivo and in vitro revealed that the early IFN-dependent response in the vagina after genital infection was independent of TLR3 (Figure 3E). Moreover, in spleen and peritoneal cells, we observed no role for TLR3 in activation of the HSV-2–induced CXCL10 response (Supplemental Figure 3, B and C), and this was also the case for the response to HSV-1 infection (Supplemental Figure 4, A and B). To examine a potential role for TLR3 in activation of adaptive immune responses after HSV-2 infection, we looked for splenic T cells at day 6 p.i. Infection led to elevation in the number of total and CD8$^+$ T cells, but with no difference between that in WT and *Tlr3*$^{-/-}$ mice (Supplemental Figure 5, A–C). Finally, we found no recruitment of CD8$^+$ cells to the lumbar medulla spinalis on day 6 p.i. in either WT or *Tlr3*$^{-/-}$ mice (Supplemental Figure 5, D–F). Thus, the observed defective control of HSV-2 infection in the CNS of *Tlr3*$^{-/-}$ mice and the associated development of disease are not due to a global defect in induction of the type I IFN response.

HSV-2 replication occurs in neurons and astrocytes in the medulla spinalis of TLR3- and IFNAR-deficient mice. The data presented above suggested that the impaired antiviral defense in *Tlr3*$^{-/-}$ mice was due to a defect in immune responses in the microenvironment at the site of viral replication, rather than being due to an overall defect in mounting innate immune responses to HSV infection in the CNS. HSV-1 and HSV-2 are neurotropic but also have the capacity to replicate in a wide range of other cell types. We therefore examined whether the defect in TLR3 mice led to a broadening of the tropism for HSV-2 in the CNS beyond neurons. Since, TLR3 is reported to be highly expressed by astrocytes (30–33), we focused on this cell type.

Immunohistochemical (IHC) analysis of lumbar medulla spinalis sections from HSV-2–infected WT mice revealed that only very few HSV-2–positive cells could be found, and most of these were neurons (NeuN$^+$) (Figure 4A). In the tissue sections from the lumbar medulla spinalis of *Tlr3*$^{-/-}$ and *Ifnar*$^{-/-}$ mice, we found many more HSV-2–positive cells, many of which were neurons. Importantly, and in contrast to the WT mice, the virus was not restricted to neurons in the *Tlr3*$^{-/-}$ and *Ifnar*$^{-/-}$ mice, and staining for astrocytes showed that this cell type was productively infected with HSV-2 in these 2 mouse strains. This was seen using antibodies against 2 different astrocyte markers: S100, which localizes to the nucleus, and glial fibrillary acidic protein (GFAP), which localizes to the cytoplasm and associates with intermediate filaments. At the infected areas of lumbar medulla spinalis — the dorsal funiculi and dorsal horn, we found 50% ± 8.3% of astrocytes were infected in *Tlr3*$^{-/-}$ mice, while only 2% ± 1.6% (P < 0.05) of astrocytes in WT mice were infected at day 6 p.i.

The data presented in Figure 2, B–D, showed that viral spread within the CNS from the medulla spinalis to the cerebellum and

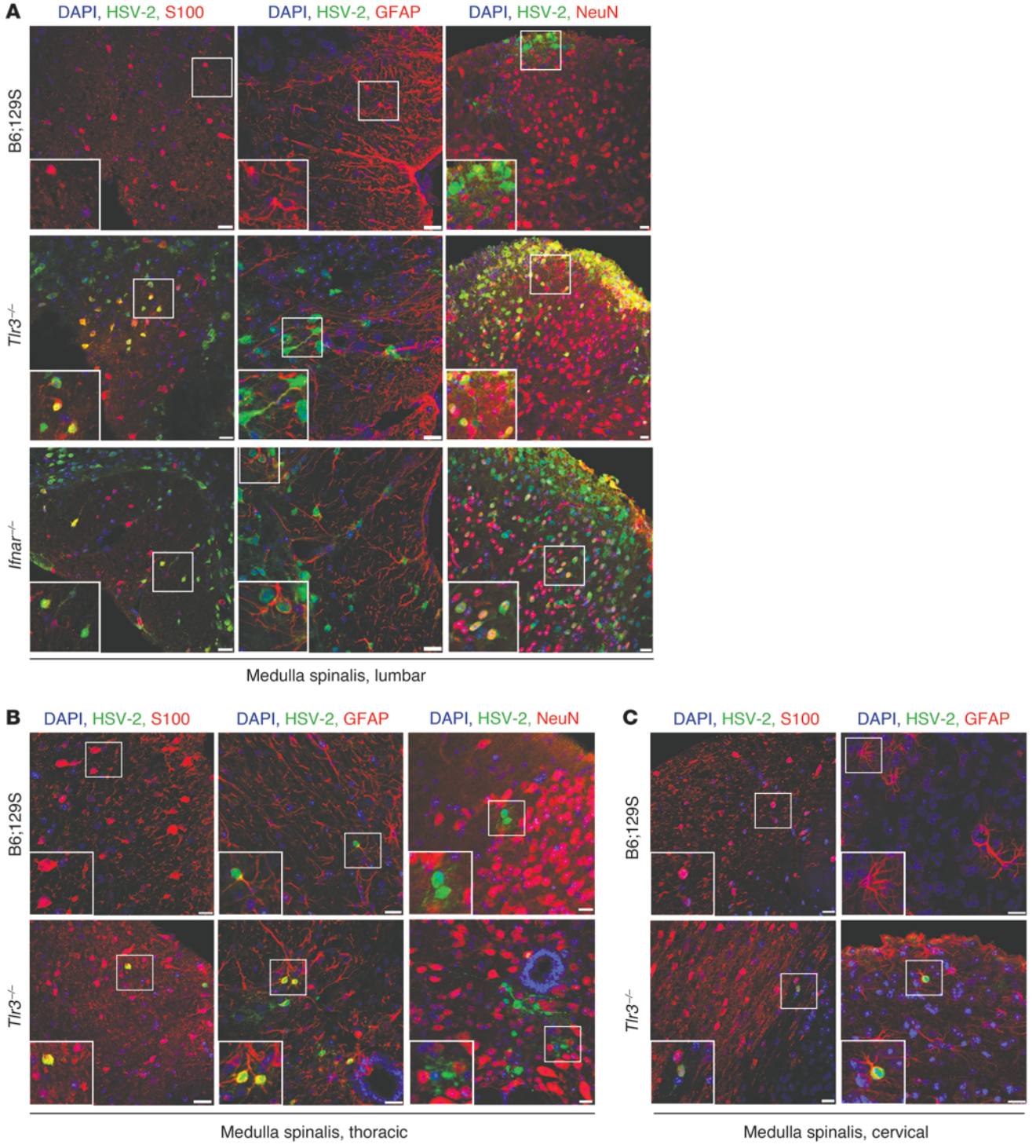

Figure 4

HSV-2 predominately infects neurons and astrocytes in the medulla spinalis of *Tlr3*$^{-/-}$ mice. (**A**) Detection of HSV-2, astrocytes, and neurons by IHC in the medulla spinalis on 6 days p.i. Dorsal funiculi or dorsal horn stained for S100 and GFAP (both markers for astrocytes), NeuN (neurons), DNA (DAPI), and HSV-2. (**B** and **C**) Costaining of thoracic and cervical regions of medulla spinalis for S100 and GFAP, NeuN, DNA, and HSV-2. Scale bar: 20 μm; magnification of insets, ×6.4. The data are reproduced twice (n = 4 mice in each group per experiment).

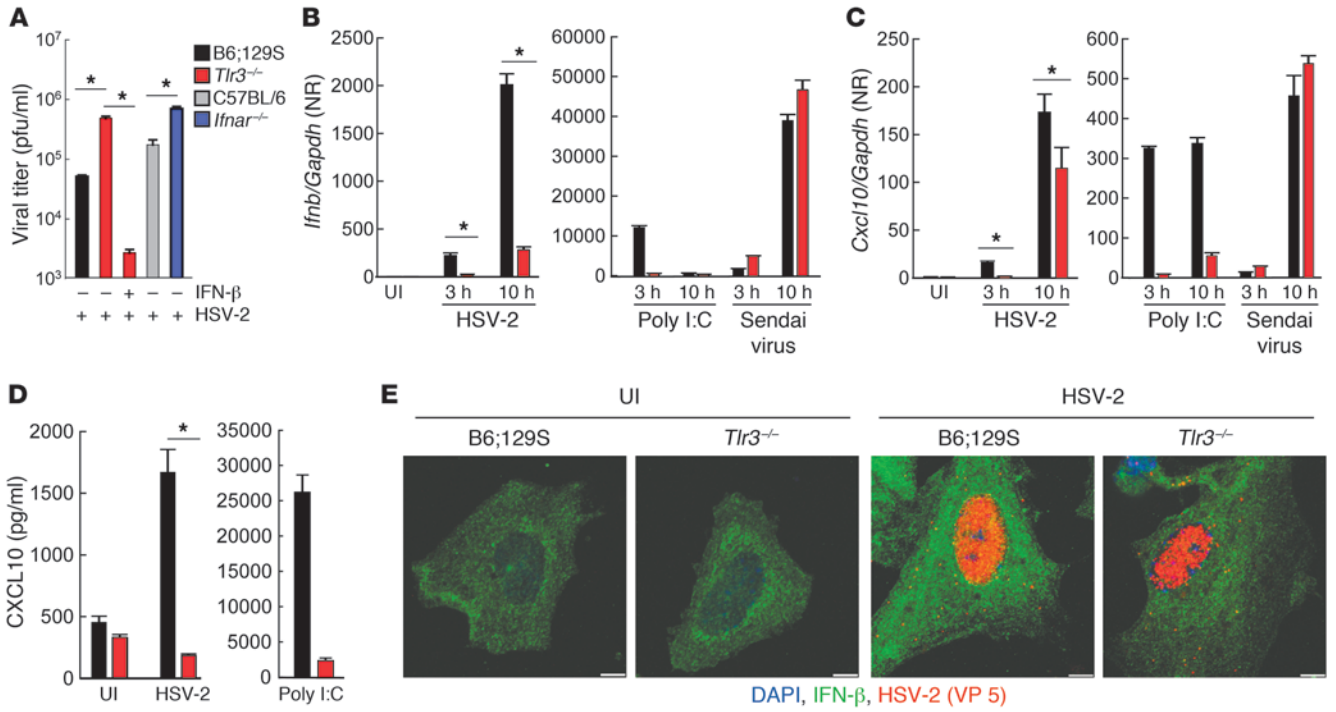

Figure 5

TLR3 is required for HSV-mediated induction of IFN-β signaling and resistance against HSV-2 infection in astrocytes. (**A**) Astrocytes were infected with 0.1 MOI of HSV-2 for 6 hours, and extracellular virus was removed by washing. Thirty hours p.i., supernatants were harvested, and viral load was determined. IFN-β (25 U/ml) was given 24 hours prior to infection. (**B** and **C**) Expression of *CXCL10* and *IFN*-β mRNA in astrocytes after HSV-2 infection (0.1 MOI), poly I:C treatment (25 μg/ml), or infection with Sendai virus (0.001 MOI). NR, normalized ratio. (**D**) CXCL10 protein expression in astrocytes 24 hours after stimuli. (**E**) Confocal images of uninfected or HSV-2–infected astrocytes (6 hours). Brefeldin A was added to the culture 1 hour p.i. The cells were stained for VP5 (red; major capsid protein), IFN-β (green), and DNA (blue; DAPI). Scale bar: 5 μm. Similar results were obtained in 3 independent experiments ($n = 3$ per group per experiment). *$P < 0.05$.

cerebrum was inefficient, with little or no virus being detected in the samples from the cerebrum, regardless the genetic background. Nevertheless, we noted that the virus spread beyond the medulla spinalis more efficiently in the *Tlr3*$^{-/-}$ mice. The amount of infected cells per section was 10 ± 3 in the thoracic part of the medulla spinalis of *Tlr3*$^{-/-}$ mice and 1 ± 2 in case of cervical part. While the virus spread inefficiently in WT mice, there were only 1 ± 2 infected cells per section in thoracic part and no cells in cervical part of the medulla spinalis. Interestingly, IHC analysis of sections from thoracic and cervical medulla spinalis revealed that in these regions HSV-2 was mainly detected in astrocytes (Figure 4, B and C). Thus, TLR3 deficiency broadens the tropism for HSV-2 in the CNS, rendering not only neurons but also astrocytes permissive to the infection.

TLR3-deficient astrocytes are defective in HSV-induced IFN-β production and exhibit elevated permissiveness to HSV-2 infection in vitro. The observed HSV tropism for astrocytes in *Tlr3*$^{-/-}$ mice led us to investigate primary astrocytes in vitro. In particular, we were interested in examining the potential relation between TLR3 and type I IFN in restriction of HSV-2 in astrocytes. We first examined whether TLR3 deficiency altered the efficiency of HSV-2 replication in astrocytes. As seen in Figure 5A, HSV-2 infection led to productive replication in astrocytes in vitro, and, importantly, a significantly higher viral yield was harvested from the supernatants of *Tlr3*$^{-/-}$ and *Ifnar*$^{-/-}$ astrocytes compared with that from WT cells. Treatment of the *Tlr3*$^{-/-}$ astrocytes with recombinant IFN-β reduced the viral titer to a level below what was seen in WT cells (Figure 5A). Examination of the ability of the astrocytes to respond to HSV-2 infection with an IFN response revealed that the infection triggered expression of IFN-β and CXCL10 RNA and protein in a manner dependent on TLR3 (Figure 5, B–E). Similarly, HSV-1–induced CXCL10 expression in astrocytes was also dependent on TLR3 (Supplemental Figure 3C).

Discussion

HSV-1 and HSV-2 belong to the group of alphaherpesviruses, which have a very broad tropism and replicate lytically in many cell types, most notably cells of the epithelial and fibroblast cell lineages. Importantly, alphaherpesviruses are neurotropic and establish latent infections in these cells after retrograde transport to the ganglia. Due to the neurotropism, alphaherpesviruses can also enter into the CNS, in which they can cause serious diseases. Our data suggest that the *Ifnar*$^{-/-}$ and *Tlr3*$^{-/-}$ mice developed myelitis after vaginal HSV-2 infection, and exhibited urinary retention, constipation, and fatty liver more commonly than WT mice.

An important task for the host is thus to restrict the access of HSV to the CNS and spread within the CNS. It has been reported that patients with defects in TLR3 are susceptible to HSV infections in the CNS (24, 26), thus suggesting a role for TLR3 in immunological control of these viruses in the peripheral tissue prior to neuroinvasion, in the peripheral nervous system, or in the CNS. Our present finding that prevention of viral replication and

spread within the CNS is impaired in TLR3-deficient mice, which display unaltered viral loads in peripheral tissue and at early stages after entry into the CNS, suggests that the role of TLR3 in HSV infection is within the CNS. We found higher viral load in the cerebellum of *Tlr3*$^{-/-}$ mice compared with that in the *Ifnar*$^{-/-}$ mice. These data indicate that TLR3 has antiviral functions in the cerebellum independent of type I IFN. One possibility is that HSV, in addition to spreading to neighboring glial and neuronal cells in the lumbal part of the medulla spinalis, may also spread via long neurons that reach the cerebellum and that this is controlled in a TLR3-dependent but type I IFN–independent way. Moreover, we present in vivo and in vitro data suggesting that *Tlr3*$^{-/-}$ astrocytes are more permissive to HSV infection and that this is due to impaired type I IFN production by this cell type in the absence of TLR3. Thus, we propose that astrocytes sense HSV entry into the CNS and mount a type I IFN response, which rapidly restricts the virus after neuronal transport into the CNS.

TLR3 is highly expressed in the CNS (Supplemental Figure 6), and several studies have examined the expression of PRRs in different cell types in the CNS. While microglia cells express most, if not all, TLRs, other glial cells and neurons are much more restricted in their pattern of TLRs (30, 31). Importantly, TLR3 is selectively expressed as the sole nucleic acid–sensing TLR on astrocytes and oligodendrocytes (Supplemental Figure 6 and refs. 30, 32, 33), and its expression is further elevated by IFN treatment and virus infections (31). Thus, the pattern of PRR expression in the CNS further suggests an important role for TLR3 in sensing viruses in the CNS. This is supported by 2 independent studies on TLR3 and West Nile virus infection (20, 21). While both reports identified key roles for TLR3 in innate recognition of West Nile virus infection, the 2 studies differ with respect to whether TLR3 plays a beneficial or deleterious role for the host during the infection.

In vitro studies with astrocytes have previously shown that HSV-1 and HSV-2 have the capacity to replicate in this cell type and that recombinant IFNs inhibit the viral propagation process (34, 35). One study has proposed a role for type III IFN in restricting HSV-1 replication in vitro in astrocytes (35). However, in our model, IFN-λ receptor deficiency did not affect development of disease in the CNS after HSV-2 infection (3). Collectively, our present work provides in vivo evidence of physiological importance for the previously reported HSV replication in astrocyte cultures, which could be inhibited by type I IFN (34). In addition, our work demonstrates that the HSV-induced IFN response in astrocytes is mediated through a TLR3-dependent pathway.

Work by Bedoui and associates has recently shown that *Tlr3*$^{-/-}$ mice have impaired development of virus-specific CD8$^+$ T cells in a model for cutaneous HSV-1 infection (28). In our model, we found similar levels of CD8$^+$ T cells in the spleen of WT and *Tlr3*$^{-/-}$ mice at day 6 after vaginal HSV-2 infection. Moreover, we did not find recruitment of CD8$^+$ T cells to the lumbar medulla spinalis (Supplemental Figure 5, D–F). These data argue against a role for the adaptive immune system in control of HSV-2 in the CNS in this model. Presently, we do not know whether the findings obtained in the current study on HSV-2 will also apply in a model for HSV-1 encephalitis after initial infection in the periphery (e.g., the ocular infection model) (36). It is of note, however, that the IFN response to HSV infection in astrocytes in vitro was dependent on TLR3 for both HSV-1 and HSV-2.

We did not find a global defect in activation of innate immune responses in *Tlr3*$^{-/-}$ mice, and we present data demonstrating that most PRRs reported to detect HSV are expressed in the CNS during HSV infection. This suggests that other HSV-sensing PRRs are still operative in the CNS and responsible for the strong innate response observed p.i. in the *Tlr3*$^{-/-}$ mice. At this stage, we cannot explain why other HSV-sensing PRRs fail to compensate for the lack of TLR3. By contrast, *Ifnar*$^{-/-}$ mice fail to induce expression of most PRRs after HSV infection (Supplemental Figure 2B), which could contribute to more severe disease development in these mice. By using an intraperitoneal infection model for HSV-1, Kurt-Jones et al. have previously reported that *Tlr2*$^{-/-}$ mice are strongly impaired in inducing an inflammatory response, which renders the mouse resistant to encephalitis in this model (10). In our model, *Tlr2* and *Tlr9* double-deficient mice were indistinguishable from WT mice with respect to expression of IFNs and inflammatory genes in the medulla spinalis. In an intranasal or corneal HSV-1 infection model, *Myd88*$^{-/-}$ mice have previously been reported to develop lethal encephalitis, mainly due to uncontrolled infection. These data suggest a complex role for TLR2 and other TLRs in the immune response to HSV infections, by contributing to both antiviral defense and immunopathology (36, 37). We have recently reported the identification of IFI16 and its murine ortholog, Ifi204, as intracellular sensors of HSV-1 DNA (17). It will be interesting to determine whether IFI16/Ifi204 or other intracellular PRRs play a role in immunological control of HSV in the CNS.

Defects in TLR3, TRAF3, and STAT1 function render humans highly susceptible to HSV-1 encephalitis (5, 23, 24), and a TLR3-deficient patient with repeated HSV-2 Mollaret meningitis has been reported (26). In this work, we report that TLR3 deficiency in mice, like that in humans, leads to impaired restriction of HSV infection in the CNS. We propose that TLR3 acts in astrocytes to sense HSV-2 infection in the CNS, leading to local autocrine and paracrine IFN-β production, which restricts the virus in the local environment in the lumbar medulla spinalis immediately after entry into the CNS.

Methods

Mice. Female mice used in this study were age matched (minimum, 8 weeks old; maximum, 12 weeks old). *Tlr3*$^{-/-}$ and WT (B6;129S) mice were purchased from The Jackson Laboratory. C57BL/6J and *Tlr2* and *Tlr9* double-deficient mice were bred at Taconic M&B, and *Ifnar*$^{-/-}$ mice on C57BL/6J background were bred at University of Southern Denmark or at University of Copenhagen.

Viruses and reagents. MEM, DMEM, Iscove's Modified Dulbecco's Media (IMDM), and RPMI 1640 growth media were obtained from BioWhittaker and supplemented with 200 IU/ml penicillin, 200 μg/ml streptomycin, and LPS-free FCS (BioWhittaker). Depo-Provera (Pfizer), Heparin (Leo Pharma), Brefeldin A (Sigma-Aldrich), IFN-β (PBL), isoflurane (Baxter), and ProLong Gold, DAPI, TRIzol, Poly I:C (all from Invitrogen) were used in the experiments described below. The viruses, HSV-2 (333 strain) and HSV-1 (KOS strain), were amplified in Vero cells and used at 0.1 MOI for in vitro stimulation. Sendai virus (SeV, Cantell strain) was used at 0.001 MOI.

Murine intravaginal HSV-2 model. For vaginal HSV-2 infection, mice were pretreated by subcutaneous injection of 2 mg Depo-Provera. Five days later, mice were anesthetized with isoflurane and inoculated intravaginally with 20 μl HSV-2 (6.7×10^4 PFUs) in IMDM or with media alone. Subsequently, mice were placed on their backs and maintained under anesthetics for 10 minutes. Vaginal fluids were collected by washing twice with 250 μl IMDM. Genitally infected mice were examined daily and scored for vaginal inflammation, neurological illness, and death. The severity of disease was graded using the following scores: 0, healthy; 1, genital erythema; 2, moderate genital inflammation; 3, purulent genital lesion and/or generally bad

condition; and 4, hind limb paralysis. Mice reaching score 4 were killed. Pathological examination was carried out for vagina, bladder, rectum, medulla spinalis, and cerebrum of mice at day 6 p.i.

Immunohistochemistry. Anesthetized mice were subjected to perfusion with 10% formalin, and cerebrum and medulla spinalis tissue were subsequently excised. Tissues were cut into sections and left in 20%–30% sucrose solution for 4 days. Sections were embedded in OCT solution (Tissue-Tek) and frozen. For H&E and $CD45^+$ staining, the tissues were postfixed in formalin and embedded in paraffin. Four-μm-thick sections were mounted on glass slides and stained with H&E. Antibody retrieval was performed in the autostainer using standard CCI solution (pH 8; Ventana Medical Systems). IHC stainings with anti-CD45 (Dako) and anti–HSV-2 (Dako) antibodies, diluted 1:100 and 1:1,000, respectively, were performed on a BenchMark XT automated slide stainer (Ventana Medical Systems) according to the manufacturer's instructions. HRP-labeled primary antibodies were visualized using UltraView Universal DAB detection system (Ventana Medical Systems) and developed with chromagen diaminobenzidine (DAB). Finally, the slides were washed in rinse water, counterstained in Mayer's hematoxylin, dehydrated, and cover slipped.

Confocal microscopy of tissue sections. For astrocyte and neuronal staining, 30-μm cryosections (HM 500 OM, Mikrom) were incubated in TEG buffer (10 mM Tris Base, 0.5 mM EGTA, pH 9) at 60°C overnight (O.N.) and subsequently treated with methanolic H_2O_2 (3% H_2O_2 and 1% absolute methanol) for 30 minutes. The sections were washed and incubated with primary antibodies at 4°C O.N., including rabbit polyclonal anti–HSV-2 (1:500; Dako), mouse anti–Neuronal Nuclei (NeuN) (1:300; Chemcon), mouse anti-GFAP (1:400; Sigma-Aldrich), and mouse anti-S100 (1:200; Abcam). The secondary antibodies, chicken anti-rabbit Alexa Fluor 488 and donkey anti-mouse Alexa Fluor 568 (Invitrogen), were used at 1:500 dilutions for 1 hour at 20°C. Nuclei were stained with DAPI. The sections were washed 5 times in 0.3% Triton-X in TBS and mounted in ProLong Gold. Stainings were imaged on a Zeiss LSM 710 laser scanning microscope, using a C-Apo 40 × 1.2 water immersion lens. Zen 2010 acquisition software and ImageJ (http://rsbweb.nih.gov/ij/) were used for making collapsed z-stacks.

Confocal microscopy of primary astrocytes. Cells grown on glass cover slips were infected with HSV-2 (6 hours). Two μg/ml Brefeldin A was added to the culture 1 hour p.i. Cells were fixed in methanol and permeabilized in 0.5% Triton X-100. Cover slips were preincubated in 5% BSA/0.05% Tween20/PBS and costained at 4°C O.N. with primary antibodies directed against IFN-β (PBL; 1:100) and VP5 (Abcam; 1:200) and secondary Alexa Fluor 488– and Alexa Fluor 647–labeled antibodies (1:500) for 1 hour. Cover slips were mounted and imaged, as described above, using a plan-apo 63 × 1.4 oil immersion lens (Zeiss).

Virus plaque assay. Organs were isolated, immediately put on dry ice, and stored at –80°C until use. Organs were thawed and homogenized in the appropriate solutions and pelleted by centrifugation at 1,600 *g* for 30 minutes. Supernatants were used for plaque assay. In the case of vaginal washes and cell supernatants, samples were used directly for plaque titration after thawing. Vero cells were seeded in 5-cm-diameter plates in MEM with 5% FCS; the next day, cells were incubated with 100 μl serial dilution of the samples with 400 μl MEM. After 1 hour, 8 ml of MEM containing 2% human immunoglobulin (CSL Behring) were added, and the plates were further incubated for 2 days. Cells were subsequently stained with 0.03% methylene blue to allow quantification of plaques.

Quantitative RT-PCR. Total RNA was extracted with TRIzol according to manufacturer's recommendations. Briefly, cells were lysed in TRIzol and chloroform was added, followed by phase separation by centrifugation. RNA was precipitated with isopropanol and pelleted by centrifugation. Pellets were washed with 80% ethanol and redissolved in RNase-free water. For cDNA generation, RNA was subjected to reverse transcription with oligo(dT) as primer and Expand reverse transcriptase (both from Roche). Before quantitative RT-PCR, RNA was treated with DNase I (Ambion) to remove any contaminating DNA, the absence of which was confirmed in control experiments in which the reverse transcriptase enzyme was omitted. The High Pure RNA Isolation Kit (Roche) was used for isolation of mRNA from primary cells. The mRNAs were quantified using SYBR Green (Stratagene) with the following primers: *Ifna*, 5′-CGGTGATGAGCTACTGGC-3′ and 5′-TTTGTACCAGGAGTGTCAAGG-3′; *Gapdh*, 5′-CAATGTGTCCGTCGTGGA-3′ and 5′-GATGCCTGCTTCACCACC-3′; *Tlr2*, 5′-GGCTCTTCTGGATCTTGGTG-3′ and 5′-GAGTCCGGAGGGAATAGAGG-3′; *Tlr3*, 5′-CTCTTGAACAACGCCCAACT-3′ and 5′-GTCCACTTCAGCCCAGAGAA-3′; *Tlr9*, 5′-CATGGACGGGAACTGCTACT-3′ and 5′-GGCACCTTTGTGAGGTTGTT-3′; *RIG-I*, 5′-ATGGCAGACAAAGAGGAGGA-3′ and 5′-TCGTGGAAGAAGGCTTTGAG-3′; *MDA5*, 5′-ACAGAGGCCTGGAACGTAGA-3′ and 5′-CTGCCCATGTTGCTGTTATG-3′; *Dai*, 5′-TTCTAGAGGACGCCACCATT-3′ and 5′-CTTCTTTCTTCGGCTCTTCA-3′; *Tnfa*, 5′-GTAGCCCACGTCGTAGCAAAC-3′ and 5′-ATCGGCTGGCACTAGTT-3′; *Ifi204*, 5′-TGGTCCCAAACAAGTGATGGTGC-3′ and 5′-TCAGTTTCAGTAGCCACGGTAGCA-3′; and *Cxcl10*, 5′CGATGACGGGCCAGTGAGAATG-3′ and 5′-TCAACACGTGGGCAGGATAGGCT-3′. The *Ifn*-β mRNA was quantified by real-time PCR using the TaqMan gene expression assay Mm00439546_s1 and TaqMan RNA-to-CT 1-Step Kit (Applied Biosystems).

ELISA measurements. 100 μl of the vaginal wash or cell culture supernatants were used to detect CXCL10, according to the instructions of the manufacturer of the Mouse CXCL10 DuoSet ELISA Development System (R&D systems).

Primary cell isolation and in vitro stimulation. For isolation of glial cells from mice, neonatal cerebra were harvested, trypsinized for 25 minutes, and filtered through a 70-μm pore size filter. Cells of 3 cerebra were then seeded on 1 uncoated 75 cm^2 culture flask and incubated with 40 ml DMEM containing 10% FCS. The medium was replenished on days 1 and 4 after plating. Henceforth, either microglia or astrocytes were isolated. Microglia were isolated using the following method: on days 12–14 of culturing, microglia were isolated by shaking the flask at 250 rpm for 48 hours; cells were then pooled, centrifuged, and seeded at appropriate densities on 96-well plates O.N. for further stimulation. Astrocytes were isolated using the following method: glial cells were passaged 2–3 times and shaken at 250 rpm for 48 hours, supernatant was eliminated, and the remaining adherent cells were predominantly astrocytes (>93%). The purity of the astrocytes was checked by flow cytometry using Alexa Fluor 488–labeled anti-GFAP antibody (Invitrogen) and confocal microscopy. Astrocytes were seeded in 24-well plates (2.4×10^5 cells/ml) and stimulated as indicated. For virus replication assay in astrocytes, cells were incubated with HSV-2 at 0.1 MOI for 6 hours. Nonadherent virus was removed by washing with DMEM. The virus content in the last wash was under the detection level in virus plaque assays. Further analysis of virus content was performed using the plaque assay described above and supernatants harvested 24 hours p.i. In some experiments, cells were treated with 25 IU/ml IFN-β 24 hours p.i.

Peritoneal and spleen cells were harvested from age-matched 6- and 12-week-old female mice. Peritoneal cells were obtained by injecting PBS containing 5% FCS and 20 IU/ml heparin into the peritoneal cavity and washed repeatedly. Cells were washed, pooled, counted, and resuspended in RPMI containing 5% FCS. Spleens were gently homogenized manually in a glass homogenizer in RPMI supplemented with 10% FCS. Erythrocytes were removed by hemolysis. The cells were passed through a 70-μm pore size filter, pooled, washed, counted, and seeded 24 hours prior to stimulation as indicated above.

Flow cytometry. The spleens were isolated as described above but not pooled. Isolation of cells from medulla spinalis was performed as isolation of neonatal cerebrum. Cells were first blocked for 15 minutes with 10% nor-

mal goat serum (Dako) or rat IgG (Jackson ImmunoResearch Inc.) to prevent nonspecific binding. For quantifying primary astrocytes cell culture, the cells were trypsinized, fixed in methanol, permeabilized in 0.5% Triton X-100, and blocked with mouse IgG (Jackson ImmunoResearch Inc.). The antibodies, anti-CD3 FITC (clone 17A2, Pharmingen), anti-CD8 PE (clone 53-6.7, eBioscience or BD Pharmingen), anti-NK1.1 APC (clone PK136, BD Pharmingen), or Alexa Fluor 488–labeled anti-GFAP antibody (Invitrogen), were added and incubated for 15 minutes at 20°C in the dark. After wash in PBS/BSA/Azide (PBS, pH 7.4, supplemented with 0.5% BSA and 0.05% sodium azide), 7-AAD Via-Probe (BD Biosciences) was used to identify dead cells. Subsequently, the cells were analyzed or sorted on a FC500 flow cytometer (Beckman Coulter) or a FACSAria III (BD Biosciences). FlowJo software version 8.8.3 (Tree Star Inc.) was used for data analysis.

Statistics. The data are shown as mean ± SEM. The statistical significance was determined by 2-tailed Student's *t* test or Wilcoxon rank sum test. For binary data, the Fisher's exact test was used. *P* values of less than 0.05 were considered to be statistically significant.

Study approval. All described animal experiments have been reviewed and approved by Danish government authorities and, hence, comply with Danish laws (The Animal Experiments Inspectorate, Slotsholmsgade 10, 1216 København K, Denmark).

Acknowledgments

The technical assistance of Kirsten Stadel Petersen and Helene Andersen is greatly appreciated. Flow cytometry and cell sorting were performed at the FACS Core Facility, the Faculty of Health Sciences, Aarhus University. This work was supported by research grants from the Danish Medical Research Council (grants no. 09-072636 and no. 10-094283), the Novo Nordisk Foundation, the Velux Foundation, the Lundbeck Foundation (grant no. R34-3855), Elvira og Rasmus Riisforts almenvelgørende Fond, and Fonden til Lægevidenskabens Fremme. L.S. Reinert is recipient of a PhD fellowship from the Faculty of Health Sciences, University of Aarhus, and K.A. Horan was funded by a Marie Curie Incoming International Fellowship.

Received for publication September 7, 2011, and accepted in revised form February 1, 2012.

Address correspondence to: Søren Riis Paludan, Department of Biomedicine, Aarhus University, Wilhelm Meyers Allé 4; DK-8000 Aarhus C, Denmark. Phone: 45.89421766; Fax: 45.87167843; E-mail: srp@microbiology.au.dk.

1. Roizman B, Knipe DM, Whitley RJ. Herpes simplex viruses. In: Knipe DM, Howley PM, eds. *Fields Virology*. 5th ed. New York, New York, USA: Lippincott–Williams and Wilkins; 2007:2501–2601.
2. Tyler KL. Herpes simplex virus infections of the central nervous system: encephalitis and meningitis, including Mollaret's. *Herpes*. 2004;11(suppl 2):57A–64A.
3. Ank N, et al. An important role for type III interferon (IFN-lambda/IL-28) in TLR-induced antiviral activity. *J Immunol*. 2008;180(4):2474–2485.
4. Biron CA, Byron KS, Sullivan JL. Severe herpesvirus infections in an adolescent without natural killer cells. *N Engl J Med*. 1989;320(26):1731–1735.
5. Dupuis S, et al. Impaired response to interferon-alpha/beta and lethal viral disease in human STAT1 deficiency. *Nat Genet*. 2003;33(3):388–391.
6. Liu T, Khanna KM, Chen X, Fink DJ, Hendricks RL. CD8(+) T cells can block herpes simplex virus type 1 (HSV-1) reactivation from latency in sensory neurons. *J Exp Med*. 2000;191(9):1459–1466.
7. Rager-Zisman B, Quan PC, Rosner M, Moller JR, Bloom BR. Role of NK cells in protection of mice against herpes simplex virus-1 infection. *J Immunol*. 1987;138(3):884–888.
8. Takeuchi O, Akira S. Pattern recognition receptors and inflammation. *Cell*. 2010;140(6):805–820.
9. Krug A, Luker GD, Barchet W, Leib DA, Akira S, Colonna M. Herpes simplex virus type 1 activates murine natural interferon-producing cells through toll-like receptor 9. *Blood*. 2004;103(4):1433–1437.
10. Kurt-Jones EA, et al. Herpes simplex virus 1 interaction with Toll-like receptor 2 contributes to lethal encephalitis. *Proc Natl Acad Sci U S A*. 2004; 101(5):1315–1320.
11. Lund J, Sato A, Akira S, Medzhitov R, Iwasaki A. Toll-like receptor 9-mediated recognition of Herpes simplex virus-2 by plasmacytoid dendritic cells. *J Exp Med*. 2003;198(3):513–520.
12. Paludan SR, Bowie AG, Horan KA, Fitzgerald KA. Recognition of herpesviruses by the innate immune system. *Nat Rev Immunol*. 2011;11(2):143–154.
13. Schulz O, et al. Toll-like receptor 3 promotes cross-priming to virus-infected cells. *Nature*. 2005; 433(7028):887–892.
14. Ablasser A, Bauernfeind F, Hartmann G, Latz E, Fitzgerald KA, Hornung V. RIG-I-dependent sensing of poly(dA:dT) through the induction of an RNA polymerase III-transcribed RNA intermediate. *Nat Immunol*. 2009;10(10):1065–1072.
15. Chiu YH, Macmillan JB, Chen ZJ. RNA polymerase III detects cytosolic DNA and induces type I interferons through the RIG-I pathway. *Cell*. 2009;138(3):576–591.
16. Takaoka A, et al. DAI (DLM-1/ZBP1) is a cytosolic DNA sensor and an activator of innate immune response. *Nature*. 2007;448(7152):501–505.
17. Unterholzner L, et al. IFI16 is an innate immune sensor for intracellular DNA. *Nat Immunol*. 2010; 11(11):997–1004.
18. McKimmie CS, Johnson N, Fooks AR, Fazakerley JK. Viruses selectively upregulate Toll-like receptors in the central nervous system. *Biochem Biophys Res Commun*. 2005;336(3):925–933.
19. Suh HS, et al. Astrocyte indoleamine 2,3-dioxygenase is induced by the TLR3 ligand poly(I:C): mechanism of induction and role in antiviral response. *J Virol*. 2007;81(18):9838–9850.
20. Daffis S, Samuel MA, Suthar MS, Gale M Jr, Diamond MS. Toll-like receptor 3 has a protective role against West Nile virus infection. *J Virol*. 2008; 82(21):10349–10358.
21. Wang T, Town T, Alexopoulou L, Anderson JF, Fikrig E, Flavell RA. Toll-like receptor 3 mediates West Nile virus entry into the brain causing lethal encephalitis. *Nat Med*. 2004;10(12):1366–1373.
22. Edelmann KH, Richardson-Burns S, Alexopoulou L, Tyler KL, Flavell RA, Oldstone MB. Does Toll-like receptor 3 play a biological role in virus infections? *Virology*. 2004;322(2):231–238.
23. Perez de Diego R, et al. Human TRAF3 adaptor molecule deficiency leads to impaired Toll-like receptor 3 response and susceptibility to herpes simplex encephalitis. *Immunity*. 2010;33(3):400–411.
24. Zhang SY, et al. TLR3 deficiency in patients with herpes simplex encephalitis. *Science*. 2007; 317(5844):1522–1527.
25. Guo Y, et al. Herpes simplex virus encephalitis in a patient with complete TLR3 deficiency: TLR3 is otherwise redundant in protective immunity. *J Exp Med*. 2011;208(10):2083–2098.
26. Willmann O, Ahmad-Nejad P, Neumaier M, Hennerici MG, Fatar M. Toll-like receptor 3 immune deficiency may be causative for HSV-2-associated mollaret meningitis. *Eur Neurol*. 2010;63(4):249–251.
27. Sørensen LN, Reinert LS, Malmgaard L, Bartholdy C, Thomsen AR, Paludan SR. TLR2 and TLR9 synergistically control herpes simplex virus infection in the brain. *J Immunol*. 2008;181(12):8604–8612.
28. Davey GM, Wojtasiak M, Proietto AI, Carbone FR, Heath WR, Bedoui S. Cutting edge: priming of CD8 T cell immunity to herpes simplex virus type 1 requires cognate TLR3 expression in vivo. *J Immunol*. 2010;184(5):2243–2246.
29. Tabeta K, et al. Toll-like receptors 9 and 3 as essential components of innate immune defense against mouse cytomegalovirus infection. *Proc Natl Acad Sci U S A*. 2004;101(10):3516–3521.
30. Bsibsi M, Ravid R, Gveric D, van Noort JM. Broad expression of Toll-like receptors in the human central nervous system. *J Neuropathol Exp Neurol*. 2002; 61(11):1013–1021.
31. Farina C, Krumbholz M, Giese T, Hartmann G, Aloisi F, Meinl E. Preferential expression and function of Toll–like receptor 3 in human astrocytes. *J Neuroimmunol*. 2005;159(1–2):12–19.
32. Carpentier PA, Begolka WS, Olson JK, Elhofy A, Karpus WJ, Miller SD. Differential activation of astrocytes by innate and adaptive immune stimuli. *Glia*. 2005;49(3):360–374.
33. Jack CS, et al. TLR signaling tailors innate immune responses in human microglia and astrocytes. *J Immunol*. 2005;175(7):4320–4330.
34. Adams O, Besken K, Oberdörfer C, MacKenzie CR, Takikawa O, Däubener W. Role of indoleamine-2,3-dioxygenase in alpha/beta and gamma interferon-mediated antiviral effects against herpes simplex virus infections. *J Virol*. 2004;78(5):2632–2636.
35. Li J, et al. Interferon lambda inhibits herpes simplex virus type I infection of human astrocytes and neurons. *Glia*. 2011;59(1):58–67.
36. Sarangi PP, Kim B, Kurt-Jones E, Rouse BT. Innate recognition network driving herpes simplex virus-induced corneal immunopathology: role of the toll pathway in early inflammatory events in stromal keratitis. *J Virol*. 2007;81(20):11128–11138.
37. Mansur DS, et al. Lethal encephalitis in myeloid differentiation factor 88-deficient mice infected with herpes simplex virus 1. *Am J Pathol*. 2005;166(5):1419–1426.